

Tracking of Polycarbonate Films using Low-energy Ions Final Report CRADA No. TC-774-94

R. G. Musket

January 24, 2018

Disclaimer

This document was prepared as an account of work sponsored by an agency of the United States government. Neither the United States government nor Lawrence Livermore National Security, LLC, nor any of their employees makes any warranty, expressed or implied, or assumes any legal liability or responsibility for the accuracy, completeness, or usefulness of any information, apparatus, product, or process disclosed, or represents that its use would not infringe privately owned rights. Reference herein to any specific commercial product, process, or service by trade name, trademark, manufacturer, or otherwise does not necessarily constitute or imply its endorsement, recommendation, or favoring by the United States government or Lawrence Livermore National Security, LLC. The views and opinions of authors expressed herein do not necessarily state or reflect those of the United States government or Lawrence Livermore National Security, LLC, and shall not be used for advertising or product endorsement purposes.

This work performed under the auspices of the U.S. Department of Energy by Lawrence Livermore National Laboratory under Contract DE-AC52-07NA27344.

Tracking of Polycarbonate Films using Low-energy Ions

R. G. Musket Lawrence Livermore National Laboratory Livermore, CA 94550

Abstract

Ion tracking is performed almost exclusively using ions with energies near or above the maximum in electronic stopping. For the present study, we have examined the results of etching ion tracks created by ions bombarding polycarbonate films with energies corresponding to stopping well below the maximum and just above the anticipated threshold for creating etchable latent tracks. Low-energy neon and argon ions with 18-60 keV/amu and fluences of about 10⁸/cm² were used to examine the limits for producing etchable tracks in polycarbonate films. By concentrating on the early stages of etching (i.e., ~20 nm < SEM hole diameter < ~100 nm), we can directly relate the energy deposition calculated for the incident ion to the creation of etchable tracks. The experimental results will be discussed with regard to the energy losses of the ions in the polycarbonate films and to the formation of continuous latent tracks through the entire thickness the films. These results have significant implications with respect to the threshold for formation of etchable tracks and to the use of low-energy ions for lithographic applications.

1. Introduction

For more than thirty years, polycarbonate foils have been used as particle detectors and in tracking studies [1-5]. The chemical formula for polycarbonate is $[(OC_6H_4)C(CH_3)_2(C_6H_4O)C)]_n$ or $C_{16}H_{14}O_3$, and it has the structure shown in Fig. 1 [6]. The two main commercially available versions of polycarbonate are Lexan and Makrolon. To improve our understanding of the potential use of polycarbonate films as resists for ion track lithography, we have examined the literature on tracking thresholds in polycarbonate and have performed experiments at energies lower than previously reported in an attempt to bracket the threshold for formation of latent tracks in Makrolon films. In this section, we describe the essence of the track formation process, summarize the relevant literature, and outline our study.

As an ion slows in a material, it loses energy by inelastic interactions with the electrons (electronic losses or electronic stopping) and, at sufficiently low velocities, by elastic collisions with the atoms (nuclear losses or nuclear stopping). When the ion velocity is sufficiently high, the ion trajectory is essentially a straight line over much of its path because the ions interact mainly with the electrons of the material. Due to statistical fluctuations in the energy deposition, continuous volumes of extended defects in the material can only be expected for high levels of energy deposition. Nuclear, or ion, tracks are cylinders of radiation damage centered on the essentially straight path of such high-velocity ions and result from the deposition of energy into electronic excitation. For polycarbonate this deposited energy results in chain scissions due to bond breaking. The tracks are termed latent tracks until they are etched to create holes in the polycarbonate.

Many studies have been undertaken to understand the details of the damage and the enhanced etching rates in the tracks (e.g., the nature and reactivity of the chemical species created). These details are only briefly outlined here because they are not the main thrust of this report. Identification of various radiolysis products and interpretation of the enhanced etching in tracks in bisphenol-A polycarbonate have been made using thermoluminescence [6] and electron spin resonance [6-9]. In essence, non-tracked polycarbonate is etched by cleavage of the carbonate linkage by hydroxide with hydrolysis of two adjacent carbonate linkages being required to release the relatively soluble bisphenolate anion from the surface [10]. The scissions in the tracks result in monomer segments at the end of a chain and would require only one cleavage. This simpler process contributes to the higher etch rate in the track. In addition the etchant can diffuse faster into the track than into the non-tracked material. A combination of these effects qualitatively explains the much higher etch rates for the tracks compared to the non-tracked material.

When latent tracks are created in polycarbonate using heavy, high-velocity ions that deposit very large amounts of energy into electronic excitation, the etching rate in the track $v_{\rm T}$ is orders of magnitude greater than that of the non-tracked material $v_{\rm C}$, indicating that the latent track can be described as a cylinder of continuous scission damage. For simple chemical etching in 3N NaOH a $v_{\rm T}/v_{\rm G}$ ratio of 390 has been measured for fission fragments [11]. Cases where $v_{\rm T}$ is only slightly greater than $v_{\rm G}$ correspond to a non-continuous latent track with regions of scissions separated by regions of non-scissioned material. For $v_T/v_G = 1+\delta$, where $\delta << 1$, there is only very sporadic scission damage along the path of the ion. For etched track cones, the sine of the cone half angle is equal to v_G/v_T . Thus, if $v_T/v_G = 10$, then the cone half angle will be about 5.7 degrees. For a 1 µm thick film on a substrate, a 5.7 degree cone angle will lead to an etched hole diameter at the top of the film being about 200 nm greater than that at the bottom of the film. Such a tapered hole may be acceptable for some lithographic applications; thus, assessing the threshold required to give $v_T/v_G = 10$ is a reasonable benchmark.

Another way to assess the continuous nature of the latent track is to determine the registration efficiency for the ions of interest. If the latent tracks are essentially continuous, then, after a short etching period, the etched track density (tracks/cm²) will equal the ion fluence (ion/cm²) (i.e., 100% registration efficiency) and both the lengths and the diameters of the etched tracks will be identical. The more sporadic the scission damage along the path of the ion, the lower the registration efficiency and the greater the range of etched lengths and diameters. A registration efficiency near zero would correspond to latent track conditions that yield $v_{\rm T}/v_{\rm G}=1+\delta$. High values of $v_{\rm T}/v_{\rm G}$ are correlated with high values of energy deposition and of registration efficiency [12].

The stopping, or energy loss rate curves for Xe, Ar, and Ne ions in polycarbonate as a function of reduced energy (MeV/amu) are shown in Fig. 2. These curves were calculated using the SRIM (i.e., Stopping and Range of Ions in Matter) code [13]. The maximum loss rates for these three ions occur at the Bragg peaks and are 88 MeV cm²/mg at 2.1 MeV/amu for Xe, 29 MeV cm²/mg at 0.69 MeV/amu for Ar, and 15 MeV cm²/mg at 0.45 MeV/amu for Ne. At these peaks the ratios of electronic to nuclear stopping are 434, 428, and 468, respectively. Thus, for ions with energies near these peak stopping values, essentially all the energy deposition is due to electronic excitation. As the energy is reduced the importance of nuclear stopping increases. For 13.6 MeV Xe (~0.10 MeV/amu) and 2 MeV Ar (~0.05 MeV/amu) the ratios of electronic to nuclear stopping are 11 and 21, respectively. As the nuclear stopping increases, higher angle scattering events become more important. Although such scattering effects must be evaluated for tracking lithography applications, this topic is beyond the scope of the present work.

Each stopping value below the Bragg peak intersects the electronic stopping curve at two different energies, termed the lower and upper energies. Over the years different approaches have been suggested to relate some aspect of the deposited energy with the threshold for creating continuous latent tracks. The original interest in knowing the threshold was to permit correlation of the observed and the calculated length of etched tracks in a material as a function of ion species and ion energy. Thus, the emphasis was on determining the etching threshold (i.e., the minimum energy deposition rate that leads to etchable tracks). Our interest is in determining the minimum energy required for a specific ion to create a continuous latent track with a sufficiently large value of $v_{\rm T}/v_{\rm G}$ throughout the thickness of a polycarbonate resist layer to be suitable for lithography. The main approaches to relating the experimental observables to the stopping of the ions have been total energy loss, primary specific ionization, and restricted energy loss.

Initially, the threshold criterion for creating continuous latent tracks was believed to be the minimum required total stopping [14], which is dominated by electronic stopping (abreviated as SE) at the upper energies. These authors measured a transition region for Lexan over which the track registration efficiency varied from unity to zero, corresponding to calculated values of ≥ 7 MeV cm² mg⁻¹ and ≤ 4 MeV cm² mg⁻¹, respectively. Thus, on a total stopping basis, the threshold at upper energies for continuous latent tracks was taken to be 7 MeV cm² mg⁻¹.

In addition to the uncertainty in the stopping as calculated by various models (variations are typically \pm 10 %), inconsistencies between the total stopping criterion and new experimental results were identified [15]. Helium ions with energies below the Bragg peak were efficiently registered in polycarbonate even though they deposited a total energy of only 2.2 MeV cm² mg⁻¹, and, although the total stopping criterion predicted that relativistic ion nuclei would give tracks in cellulose nitrate, none could be found. Consequently, these authors developed a semi-quantitative model of track formation that predicted a critical value of the primary specific ionization (i.e., PI), which is the number of ions formed per unit distance along the particle path, was required for creation of continuous latent tracks. They showed, on a relative basis, that their model fit data for Lexan, mica, and cellulose nitrate. The model worked well for ions with 1 < Z < 18 and 0.03 <MeV/amu < 10 and predicted a primary ionization threshold of about seven ions per unit distance (arbitrary) along the ion path. Unfortunately, their expression for the effective charge for ions was valid only for velocities above $2.5 \times 10^{-3} \, \text{Z}^{2/3}$ c, which corresponds to Ar ions with energies > 5.57 MeV and MeV/amu > 0.14. We could have extended their calculation to lower velocities using a more modern version of the velocity dependence of the effective charge of the ion [13], but we concentrated on the experimental measurements of the threshold.

The third often used method to relate the energy deposition rate to the threshold for track formation is the restricted energy loss (i.e., REL) method [16]. The REL includes only that portion of the total energy loss that produces delta rays (i.e., electrons) of less than some specified energy (usually < 350 eV). Because this method relies on a calculation of both the electronic stopping and the energy distribution of electrons, there is additional uncertainty in the calculation compared to the total electronic stopping method. For ions with energies well below the Bragg peak the electron energies are smaller and the REL approach should give results similar to that of the SE approach. Typically, the REL threshold for creating etchable latent tracks is taken to be that value giving $v_{\rm T}/v_{\rm G}=1+\delta$. In practice, the track etch rate is determined as a function of the REL, and the threshold REL is assessed by extrapolation of the data to $v_{\rm T}/v_{\rm G}=1+\delta$.

For ions with energies above the Bragg peak, this approach should yield results comparable to those obtained using very low registration efficiency criteria, because the chain scission damage is not continuous along the latent track. For ions below the Bragg peak the REL threshold determined in this way corresponds to very low energy ions that deposit their energy mainly into elastic atomic displacements. This is a consequence of the fact that even very low energy ions cause radiation damage and chain scission only at the surface and, thus, slightly enhanced etching rates over very shallow depths. Detection of such "tracks" at surfaces of non-etched or very slightly etched material leads to the smallest values for the threshold. However, such "tracks" are not useful for ion tracking lithography and will not be discussed further here.

A summary of the relevant literature for the various thresholds determined for polycarbonate materials is given in Table 1. From the results shown in this table, we can draw two main conclusions: (a) 100% registration has been reported for SE = 7 to 8 MeV cm²/mg and REL = ~3 MeV cm²/mg; and (b) for the $v_{\rm T}/v_{\rm G}$ = 10 criterion, SE = 9 to 16 MeV cm²/mg and REL = 5 to 10.6 MeV cm²/mg were required to create a readily etchable latent track. Because we expect that SE approaches REL for the low energy ions of interest here, a reasonable assumption is that the SE threshold for low energy ions for useful lithograph is in the range of 5 to 10 MeV cm²/mg.

Thus, we had planned to study the etching of polycarbonate films irradiated with Ne and Ar ions that initially deposit energy densities within this range, but due to our limited resources for these studies, we decided that we must narrow the energy deposition range to obtain some reasonable definition of the threshold. From the data reproduced in Fig. 3, the threshold for track registration was between 5 and 7 MeV cm²/mg. We concluded that the threshold for easily etchable latent tracks would be slightly higher and limited

our exploration to the range of 6 to 8 MeV cm²/mg using low-energy neon and argon ions with 18-60 keV/amu. The basic idea was to determine the threshold for the formation of etchable latent tracks by detection after minimal etching. Once this threshold (and ion energy) is determined we can then calculate the minimum ion energy incident upon a polycarbonate film such that the ion still creates an etchable latent track at the film/substrate interface.

2. Experimental considerations

Using TRIM (an earlier version of SRIM) we determined the energies of the Ne and Ar ions required to deposit SE values of about 6, 6.5, 7, 7.5, and 8 MeV cm²/mg as the ion entered the surface of the polycarbonate. The required energies were 0.80, 0.90, 1.00, 1.10, and 1.20 MeV for Ne and 0.70, 0.82, 0.94, 1.05, and 1.16 MeV for Ar. In addition, we included tracking with 2 MeV Ar, which initially deposits an SE ~ 11 MeV cm²/mg (Fig. 2a), and 13.6 MeV Xe, which initially deposits SE ~ 22 MeV cm²/mg (Fig. 2b). At the time of this 1996 study, the 2 MeV Ar was the ion planned for the new irradiation tool for CTC and the 13.6 MeV Xe was the ion used for standard irradiations of polycarbonate films at LLNL.

For this study approximately 600-nm thick Makrolon polycarbonate films were deposited on chromium films on 100-mm diameter glass substrates at CTC using the then standard deposition and baking procedures (circa early 1996). An approximately 50 mm X 50 mm square near the center of the polycarbonate film was irradiated at LLNL using a magnetically analyzed, electrostatically rastered beam of Ne⁺, Ar⁺, or Xe⁺⁴ ions obtained by ionizing the appropriate noble gas in a cold cathode ion source and accelerating the ions through a potential to achieve the desired energy. The ions were incident along the surface normal (±2°). Typical beam currents were 0.1 to 7.0 nA with the dosimetry being determined by the average fluence received in an array of four Faraday cups located outside the corners of a 50 mm X 50 mm aperture carbon mask in front of the substrates. Fluence values were about 10⁸ atoms/cm².

The uniformity of the irradiations was achieved by rastering the approximately 1 cm diameter beam over an area greater than the 50 mm X 50 mm aperture for a minimum of 10 s and was then assessed by comparing the fluence collected in each of the four Faraday cups inside the corners of the rastered area. The maximum deviation in any one cup from the average fluence in the four cups during the irradiations was <5%. Uniform irradiation should have led to etchable tracks in the films with track densities equal to the measured fluences, indicating unity probability of track formation. Unfortunately, the SEM fluences were either equal to or greater than the measured fluences, indicating that there was some bombardment by neutralized ions, which were not measured by the dosimetry system.

Consequently, we could not draw any conclusions about the track registration efficiency of the ions.

The stability of latent tracks and their susceptibility to etching can be enhanced by exposure to ultraviolet (UV) radiation in air or oxygen [24,25]. In our work, the area having latent tracks was uniformly exposed to 205 nm radiation in air for about 15 minutes with a power of 20 mW/cm². Etching of the ion-irradiated and UV-exposed polycarbonate films was accomplished in a 6 M solution of high-purity potassium hydroxide (KOH) for various times at a temperature of about 22 C. Each etching for a given time was limited to a circular area of about 38 mm² using a glass tube with an o-ring at the end to allow multiple etching experiments on the same irradiated film. For each irradiated film, the etching times were generally 1, 2, 4, 6, 8, and 10 minutes. The etching was stopped by removal from the KOH solution and rinsing in de-ionized water. Figure 4 shows a substrate with a tracked film that has been etched in isolated spots for various times. The circular spots had different colors caused by optical interference effects related to the variation of remaining film thickness.

3. Results and discussion

Images of the etched hole diameters were obtained as a function of etching time using low-energy SEM at near normal incidence. The cylindrical hole diameter was taken to be the diameter of the dark hole as determined using the calibrated markers in both the X and Y directions of the micrograph. An example of this measurement scheme is shown in Fig. 5. A sequence of SEMs showing the effects of increasing the etching time from one to eight minutes is displayed in Fig. 6. Although the largest percentage errors occur for the smallest hole diameters, no effort has been made to assess such measurements errors as a function of hole diameter. The largest errors are believed to be associated with the reproducibility of the etching process parameters, including initial surface cleanliness, substrate and etchant temperature, and timing of the etch start and stop. In addition, the variability of the thicknesses of the carbon coatings was believed to be a contributor to errors for the smallest holes.

A comparison of the hole diameter as a function of etching time for 2 MeV Ar and 13.6 MeV Xe is given in Fig. 7. Recall that both these ions deposit energy well above the threshold for creation of etchable tracks. Individual lines were fitted to the two separate sets of data using linear regression with the fitted lines as displayed. All five data points (1-10 minutes etching) for Ar were used for the fitting, and ten data points (1-16 minutes etching) were used for fitting the Xe data. R^2 is a measure of the reliability of the fit with $R^2 = 1$ being a perfect fit. Extrapolations of these fits to zero time suggest latent track diameters of about 16 nm for the Xe and 3 nm for the Ar. However, assuming the measured diameters for the small holes are accurate, these

values are upper limits on the diameter for the latent tracks, which etch very rapidly. Note that after 8 and 10 minutes of etching, the hole diameters for the two ions are almost identical because any effect of the latent track diameter has been removed. We have concluded that the two sets of data are essentially the same considering the reproducibility of the experiments.

The dependence of the hole diameter as a function of etching time for Ar ions with various energies is shown is Fig. 8(a). Because all of these ions created etchable tracks, they all deposited energy above the SE threshold, which must be <6 MeV cm²/mg. The hole diameter generally increases with etching time for each Ar energy. We repeated some of the etching steps on all five of the low energy samples for a total of fourteen repeat etchings. Of the fourteen, four results changed from no detectable holes to holes with measurable diameters, which are included in the figure. In one case the results changed from measurable holes to no detectable holes. For the nine other cases, the average reproducibility of the hole diameters was ±11% with variations of 0.5% to 22%. The reasons for these discrepancies are not clear, but issues related to the reproducibility of the etching process parameters, especially surface cleanliness, are suspected.

Figure 8(b) is a reploting the data of Fig. 8(a) showing the dependence of the hole diameter on Ar energy with etching time as the parameter. In addition, individual lines were fitted to each separate set of etch-time data using linear regression as displayed. For an individual etching time the scatter is sometimes large, but the trend is clear. Except for the 1 minute etching, all the other etching times show a slight increase in hole diameter with Ar energy. However, if we restrict the plot to Ar energies of 0.7-1.16 MeV, the hole diameter is essentially independent of Ar energy.

For Ne ions with various energies, the dependence of the hole diameter as a function of etching time is shown is Fig. 9(a). As with the Ar ions above, all of these ions created etchable tracks and the hole diameter generally increased with etching time for each Ne energy. Thus, all these ions deposited energy above the SE threshold, which must be <6 MeV cm²/mg.

A reploting of the data of Fig. 9(a) is presented in Fig. 9(b), which shows the dependence of the hole diameter on Ne energy with etching time as the parameter. As for Ar above, individual lines were fitted to the each separate set of etch-time data (except that for 1 minute) using linear regression. However, in agreement with the low-energy Ar data, the etched hole diameter does not change significantly with Ne energy.

Although additional experiments with lower energy Ar and/or Ne ions are needed to actually determine the threshold for creation of etchable tracks, we have learned that the SE threshold is <6 MeV cm²/mg. Thus, Ar ions should be suitable for ion track lithography of polycarbonate films in all cases where

the Ar deposits more than this threshold amount of energy in the film at the film/substrate interface after the ion has lost energy in passing through the film. From SRIM calculations, a 2 MeV Ar ion incident on the 600-nm thick polycarbonate film would have its energy reduced to about 1.23 MeV at the film/substrate interface where it would deposit about 8.28 MeV cm²/mg. Thus, we would expect that 2 MeV Ar would create an etchable latent track throughout the polycarbonate film.

In Fig. 10(a) the holes resulting from 10 minutes of etching of polycarbonate irradiated with 2 MeV Ar can be seen to be quite uniform in size. To verify that the 107-nm diameter holes found were really cylinders throughout the thickness of the film, we prepared cross-sectional samples for SEM analysis by pulling the film off in some areas. The micrographs shown in Fig. 10(b) and 10(c) were taken at different locations along tear lines to show the general features. As expected the holes are nearly cylindrical in shape throughout the thickness of the film. After examining many cross-sectional areas, we could only find through holes; there was no evidence of holes that did not penetrate the film. The oscillations inside the diameters of the holes throughout the thickness of the film is due presumably to the pattern of enhanced sensitivity to etching created by the standing waves from the UV radiation interacting with the film.

4. Concluding Remarks

We have examined the results of etching ion tracks created by ions bombarding polycarbonate films with energies corresponding to stopping just above the anticipated threshold for creating etchable latent tracks. Lowenergy neon and argon ions with 18-60 keV/amu and fluences of about $10^8/\text{cm}^2$ were used to examine the limits for producing etchable tracks in polycarbonate films. Although additional experiments with lower energy Ar and/or Ne ions are needed to actually determine the threshold for creation of etchable tracks, we have learned that the SE threshold is <6 MeV cm²/mg. Furthermore, improved control of the etching parameters should permit higher reproducibility of the etching studies and better assessment of any trends with ion energy.

Using cross-sectional SEM we found that an energy deposition of about 8.28 MeV cm²/mg in the polycarbonate at the film/substrate interface is sufficient to ensure that the etched structure will be nearly cylindrical in shape throughout the film thickness. Under the assumption that the threshold for creating etchable latent tracks in polycarbonate is conservatively 6 MeV cm²/mg, we used SRIM to calculate the maximum thickness of polycarbonate film that can be tracked using Ar ions of various energies. For 2, 1.8, and 1.6 MeV Ar the trackable thicknesses are 1.15, 1.01, and 0.86 μ m, respectively. However, as mentioned above, at lower energies the effect of the nuclear stopping increases and higher angle scattering events become more

important. In any case, the present results have significant implications with respect to the threshold for formation of etchable tracks and to the use of low-energy ions for lithographic applications.

It is a pleasure to acknowledge R. J. Contolini for initial discussions and planning of this work and for defining the etching procedures, R. G. Patterson for doing most of the irradiations, L. A. Tarte for performing the etching experiments, and J. M. Yoshiyama for the SEM measurements, and A. Johnson of Candescent Technologies Corporation for the preparation of the samples. Work performed under the auspices of the U. S. Department of Energy by the Lawrence Livermore National Laboratory under contract W-7405-ENG-48, including CRADA TC-774-94 with Candescent Technologies Corporation.

5. References

- 1. R. L. Fleischer, P. B. Price, and R. M. Walker, *Nuclear Tracks in Solids: Principles and Applications* (University of California Press, Berkeley, CA, 1975).
- 2. S. A. Durrani and R. K. Bull, Solid State Nuclear Track Detection: Principles, Methods, and Applications (Pergamon Press, New York, 1987).
- 3. R. Spohr, Ion Tracks and Microtechnology: Principles and Applications (Vieweg, Braunschweig, Germany, 1990)
- 4. R. L. Fleischer, Tracks to Innovation: Nuclear Tracks in Science and Technology (Springer-Verlag, New York, 1998)
- 5. W. Enge, Rad. Meas. 25, 11 (1995).
- 6. E. A. Edmonds and S. A. Durrani, Nucl. Tracks 3, 3 (1979).
- 7. S. L. Koul and I. D. Campbell, Rad. Eff. 97, 321 (1986).
- 8. E. Ferain and R. Legras, Rad. Eff. Def. Solids 126, 243 (1993).
- 9. M. I. Chipara, V. V. Grecu, P. V. Notingher, J. R. Romero, and M. D. Chipara, Nucl. Instr. and Meth. B 88, 418 (1994).
- 10. T. A. Gruhn and E. V. Benton, in *Solid State Nuclear Track Detectors*, P. H. Fowler and V. M. Clapham (eds) (Pergamon, New York, 1981), p69.
- 11. W. DeSorbo, Nucl. Tracks 3, 13 (1979).
- 12. R. L. Fleischer, in *Progress in Materials Science* (*Chalmers Anniversary Issue*), J. W. Christian, P. Haasen, and T. B. Massalki (eds) (Pergamon Press, New York, 1981), p.97.
- 13. J. F. Ziegler, Rev. Appl. Phys., J. Appl. Phys., 85, 1249 (1999).
- 14. R. L. Fleischer, P. B. Price, R. M. Walker, and E. L. Hubbard, Phys. Rev. 133, A1443 (1964).
- 15. R. L. Fleischer, P. B. Price, R. M. Walker, and E. L. Hubbard, Phys. Rev. 156, 353 (1967).
- 16. E. V. Benton and W. D. Nix, Nucl. Instr. and Meth. 67, 343 (1969).

- 17. M. Debeauvais, R. Stein, J. Ralarosy, and P. Cuer, Nucl. Phys. A90, 186 (1967).
- 18. R. P. Henke, E. V. Benton, and H. H. Heckman, Rad. Eff. 3, 43 (1970).
- 19. G. Somogyi, K. Grabisch, R. Scherzer, and W. Enge, Nucl. Instr. and Meth. 134, 129 (1976).
- 20. K. K. Dwivedi and S. Mukherji, Nucl. Instr. and Meth. 159, 433 (1979).
- 21. S. M. Farid and A. P. Sharma, Ind. J. Pure Appl. Phys. 22, 133 (1984).
- 22. Singh, S. Devi, S. Singh, and H. S. Virk, Nucl. Tracks 12, 383 (1986).
- 23. S. Ghosh, A. Saxena, and K. K. Dwivedi, Pramana-J. Phys. (India) 31, 197 (1988).
- 24. R.P. Henke, E.V. Benton and H.H. Heckman, Radiat. Eff. 3, 43 (1970).
- 25. W. de Sorbo, Nucl. Tracks 3, 13 (1979).

Table 1. Literature values for critical energy deposition for track formation

Material	Method used	Side of Bragg Pk	Critical energy deposition	Ref.
Lexan	100 % Registration	High	$SE = 7 \text{ MeV cm}^2 \text{ mg}^{-1}$	14
Lexan	100 % Registration	High & low	PI = 7 ions/unit length	15
Lexan	100% Registration?	High & low	$REL = 3.3 \text{ MeV cm}^2 \text{ mg}^{-1}$	16
Makrofol	100 % Registration?	High	$SE = 8 \text{ MeV cm}^2 \text{ mg}^{-1}$	17
Lexan "	$v_{\rm T}/v_{\rm G} = 1$ $v_{\rm T}/v_{\rm G} = 10$	High & low	REL = $2.0 \text{ MeV cm}^2 \text{ mg}^{-1}$ REL = $8.2 \text{ MeV cm}^2 \text{ mg}^{-1}$	18
Lexan "	$v_{\rm T}/v_{\rm G} = 1$ $v_{\rm T}/v_{\rm G} = 10$	High & low	REL = 1 to 2 MeV cm ² mg ⁻¹ REL = 5 to 8 MeV cm ² mg ⁻¹	19
Lexan "	$v_{\rm T}/v_{\rm G} = 1$ $v_{\rm T}/v_{\rm G} = 10$	High & low	$SE = 7.5 \text{ MeV cm}^2 \text{ mg}^{-1}$ $SE = 13 \text{ MeV cm}^2 \text{ mg}^{-1}$	20
Makrofol "	$v_{\rm T}/v_{\rm G} = 1$ $v_{\rm T}/v_{\rm G} = 9.5$	High & low	$SE = 4.9 \text{ MeV cm}^2 \text{ mg}^{-1}$ $SE = 8.9 \text{ MeV cm}^2 \text{ mg}^{-1}$	21
Makrofol "	$v_{\rm T}/v_{\rm G} = 1$ $v_{\rm T}/v_{\rm G} = 10$	High & low	REL = $4.3 \text{ MeV cm}^2 \text{ mg}^{-1}$ REL = $10.6 \text{ MeV cm}^2 \text{ mg}^{-1}$	22
Lexan "	$v_{\rm T}/v_{\rm G} = 1$ $v_{\rm T}/v_{\rm G} = 10$	High & low	$SE = 5.0 \text{ MeV cm}^2 \text{ mg}^{-1}$ $SE = 16 \text{ MeV cm}^2 \text{ mg}^{-1}$	23

Legend:

SE = Total electronic stopping PI = Primary ionization REL = Restricted energy loss

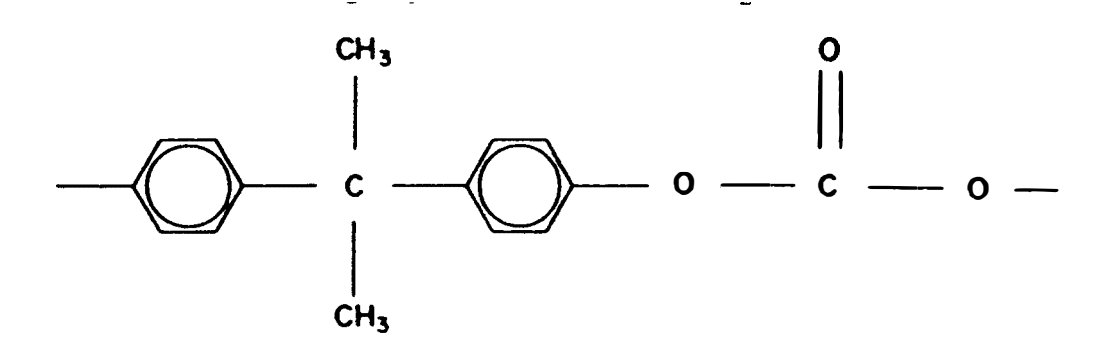


Figure 1: Structural formula of polycarbonate, $C_{16}H_{14}O_3$.

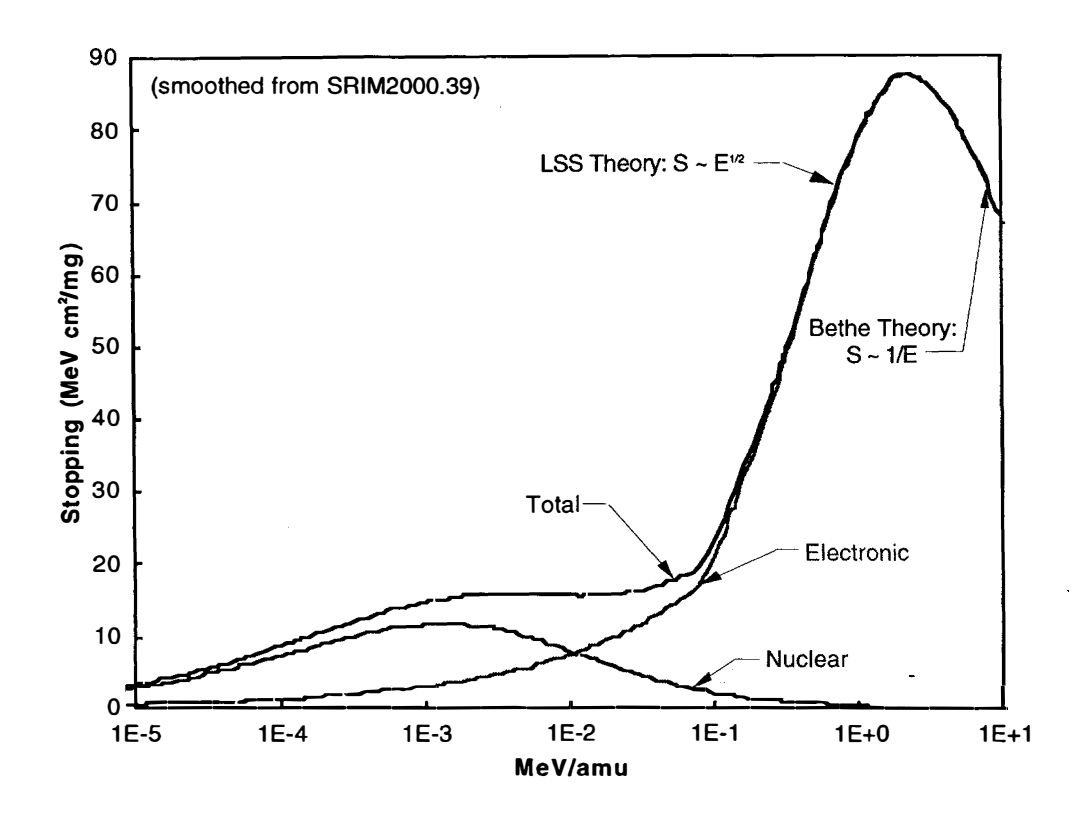


Figure 2(a): Calculated stopping of Xe in polycarbonate.

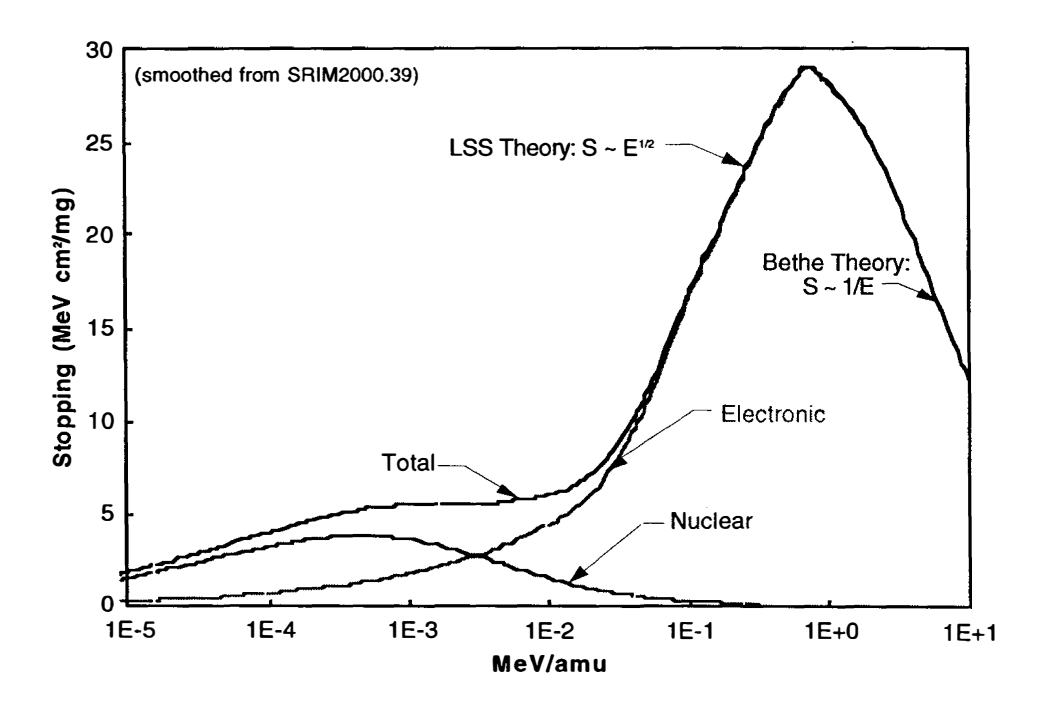


Figure 2(b): Calculated stopping of Ar in polycarbonate.

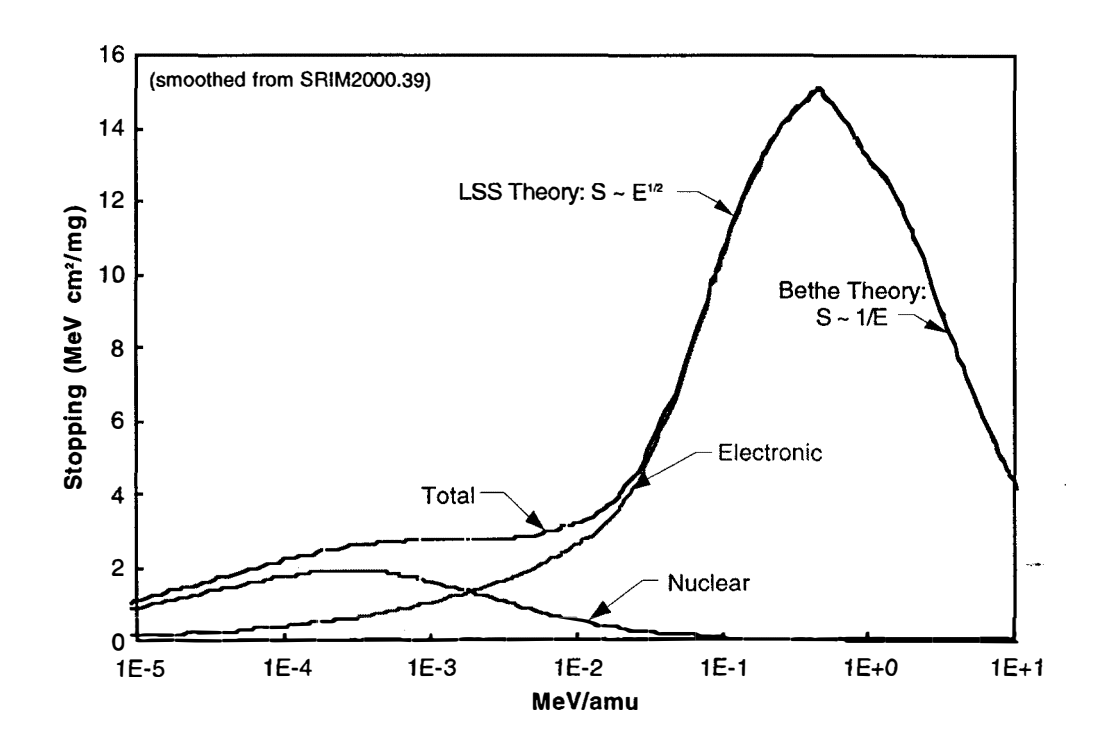


Figure 2(c): Calculated stopping of Ne in polycarbonate.

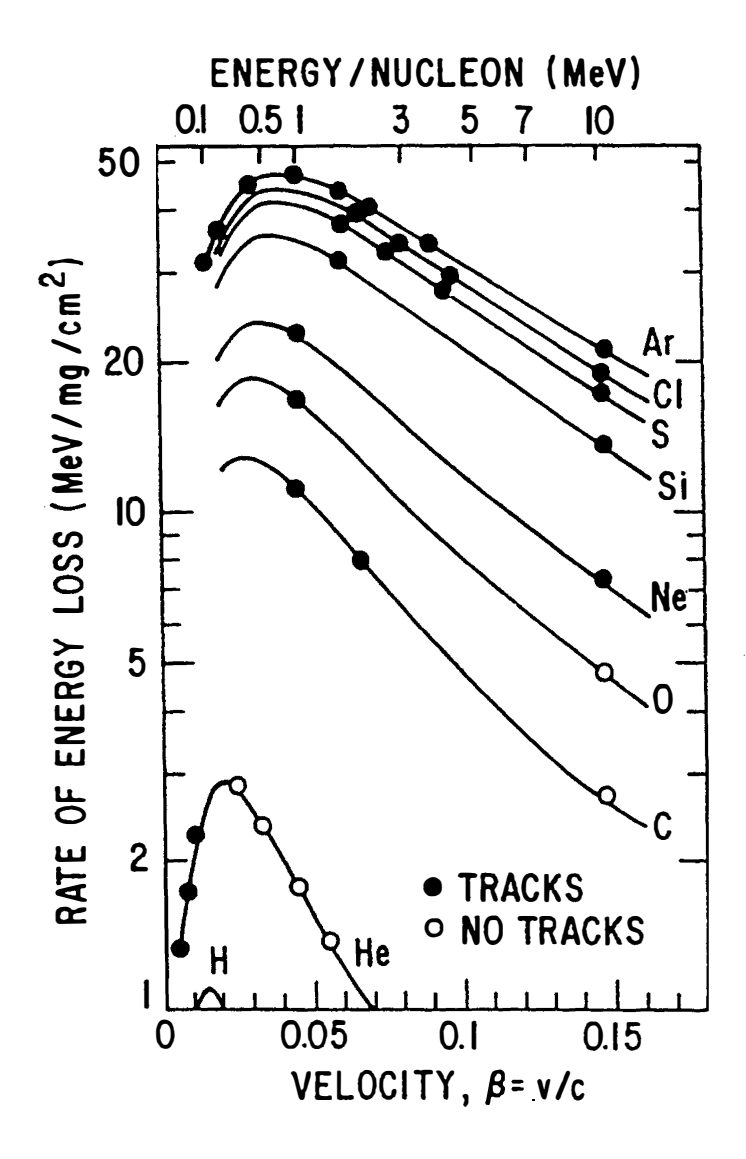


Figure 3: Efficiency of ion track registration in polycarbonate depends on the rate of energy loss for ions with Z > 5, but not for He ions [15]. The open and filled circles correspond to zero and 100% registration efficiency after etching, respectively.

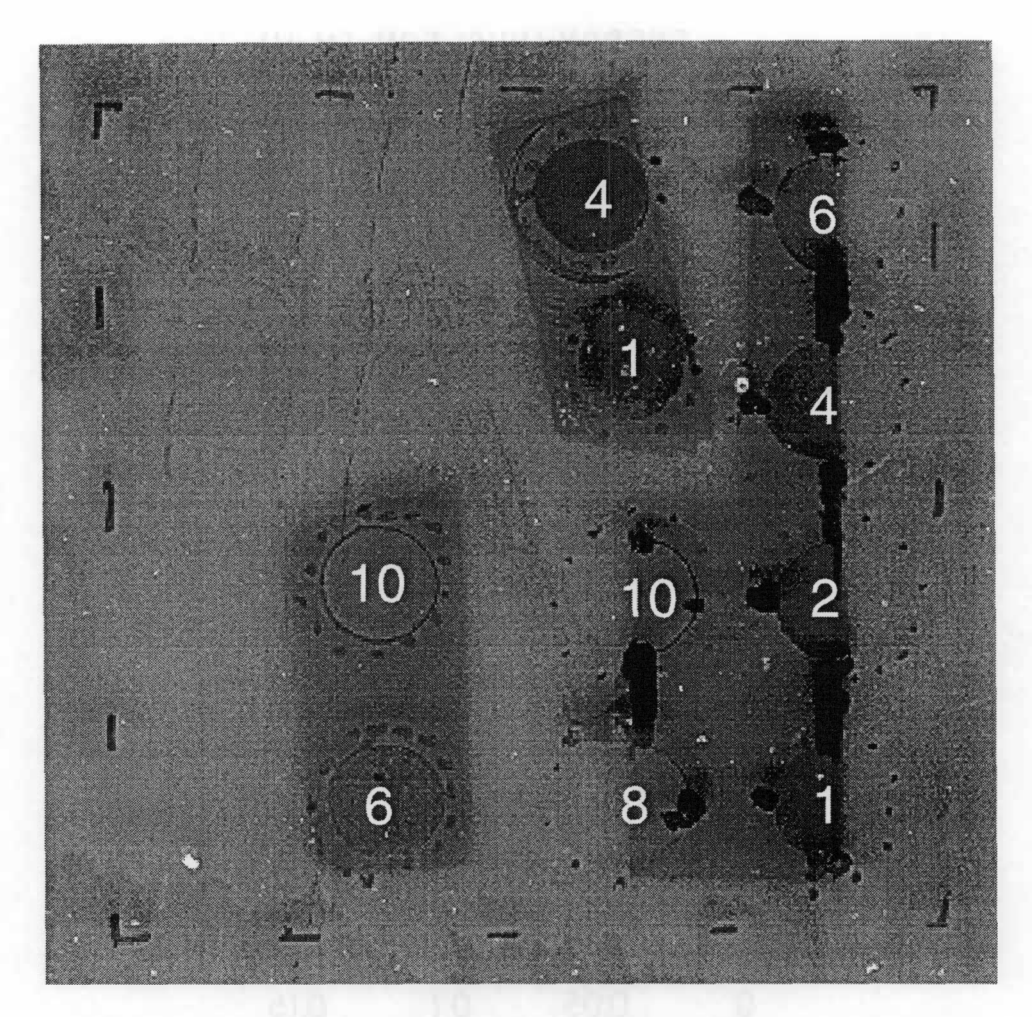


Figure 4: Sample irradiated inside dashed square (~50 mm X 50 mm) with 1.16 MeV Ar ions to a fluence of ~10⁸ Ar/cm². Numbers indicate the etching times for each etched spot (~ 7-mm diameter). The irregular rectangular areas are the areas coated with carbon for the high-resolution SEM measurements.

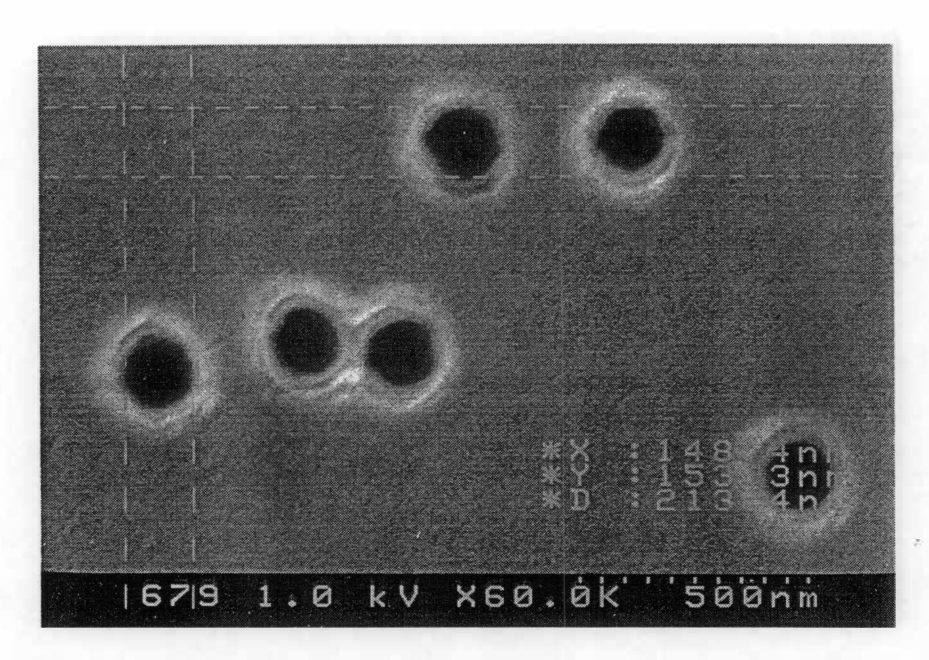


Figure 5: Typical SEM of etched holes in a polycarbonate film showing the calibrated spread between the cursors in the X and Y directions of a sample irradiated with 13.6 MeV Xe and etched for 16 minutes to yield hole diameters of about 151 nm.

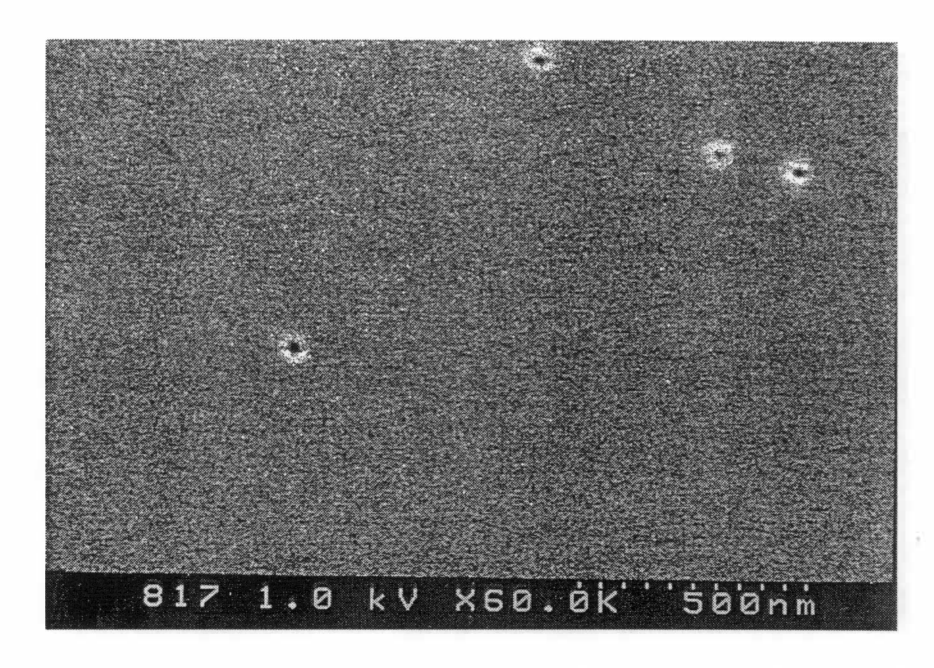


Figure 6(a): SEM showing 19 nm diameter holes in polycarbonate film after irradiation with 13.6 MeV Xe and etching for 1 minute.

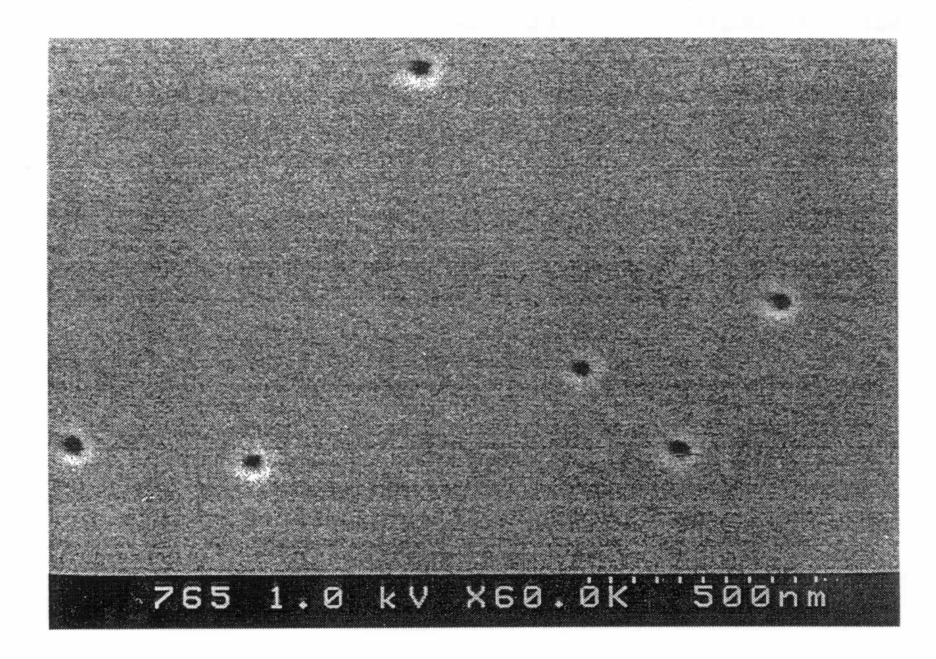


Figure 6(b): SEM showing 41 nm diameter holes in polycarbonate film after irradiation with 13.6 MeV Xe and etching for 2 minutes.

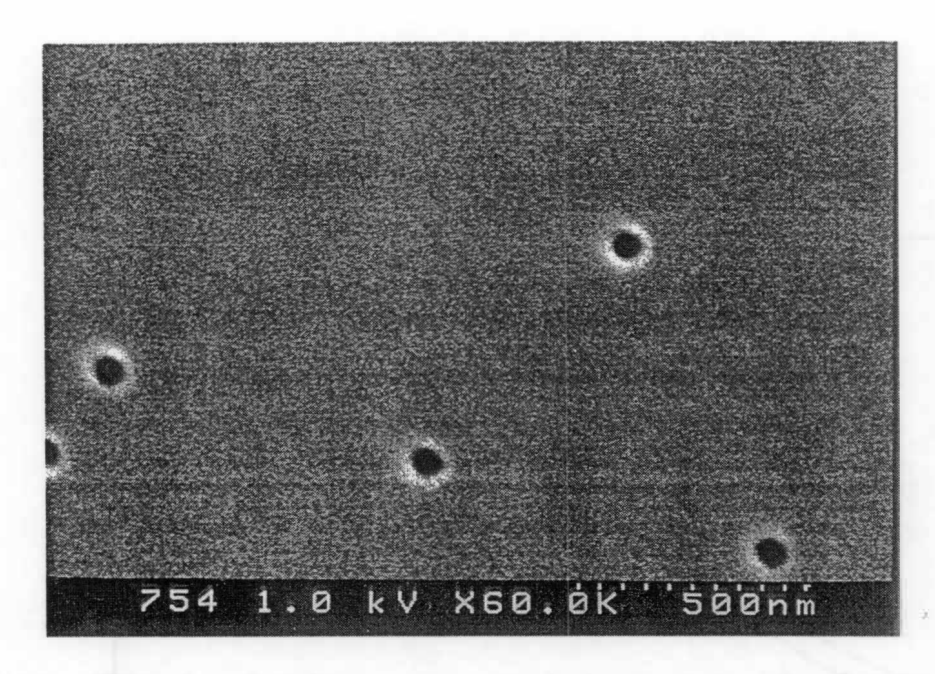


Figure 6(c): SEM showing 56 nm diameter holes in polycarbonate film after irradiation with 13.6 MeV Xe and etching for 4 minutes.

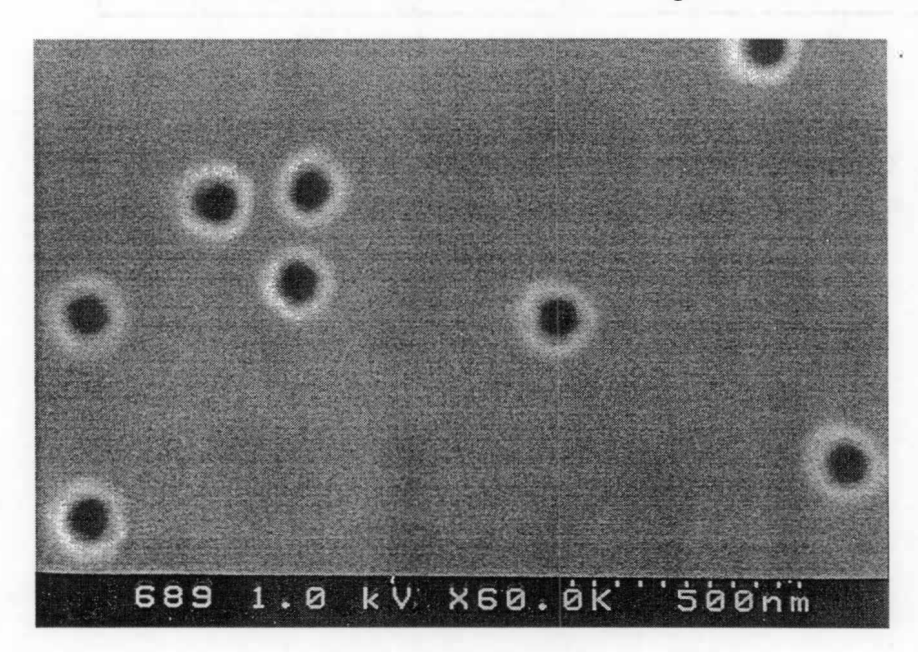


Figure 6(d): SEM showing 81 nm diameter holes in polycarbonate film after irradiation with 13.6 MeV Xe and etching for 8 minutes.

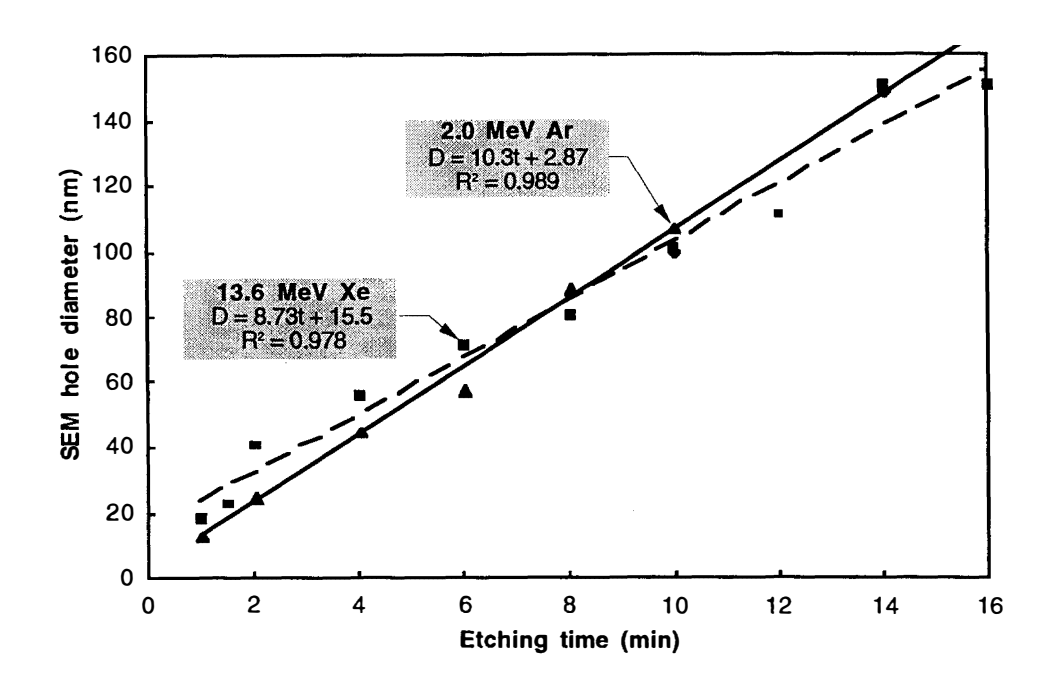
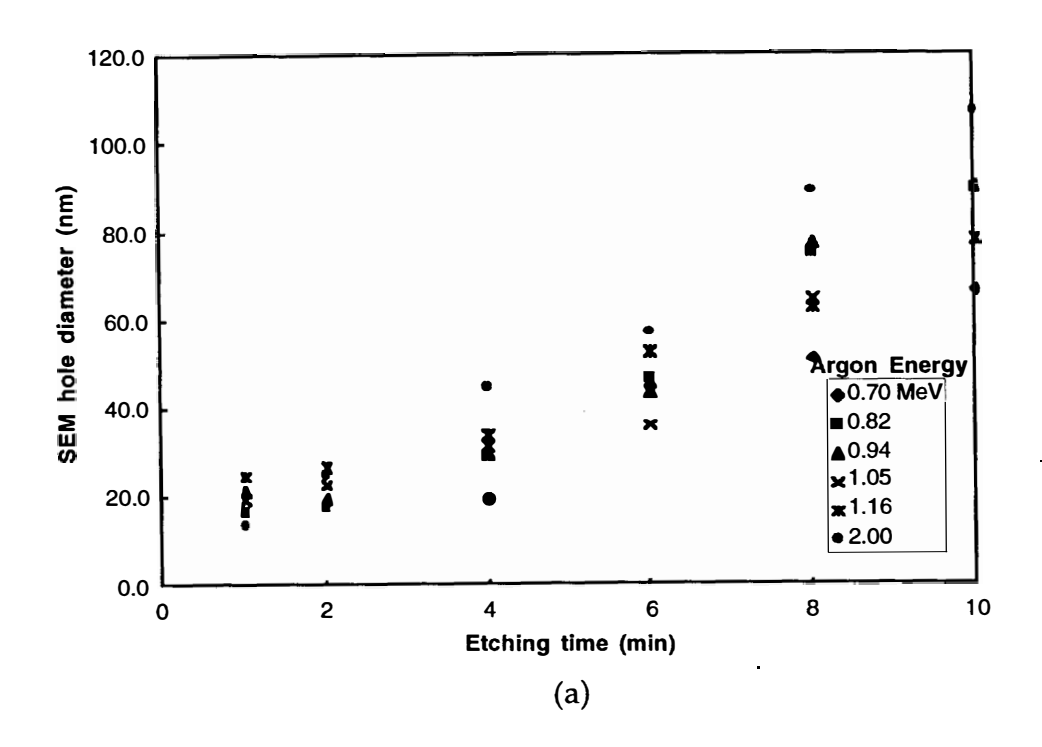


Figure 7: Comparison of hole diameters in polycarbonate films after irradiation with Ar or Xe ions and etching.



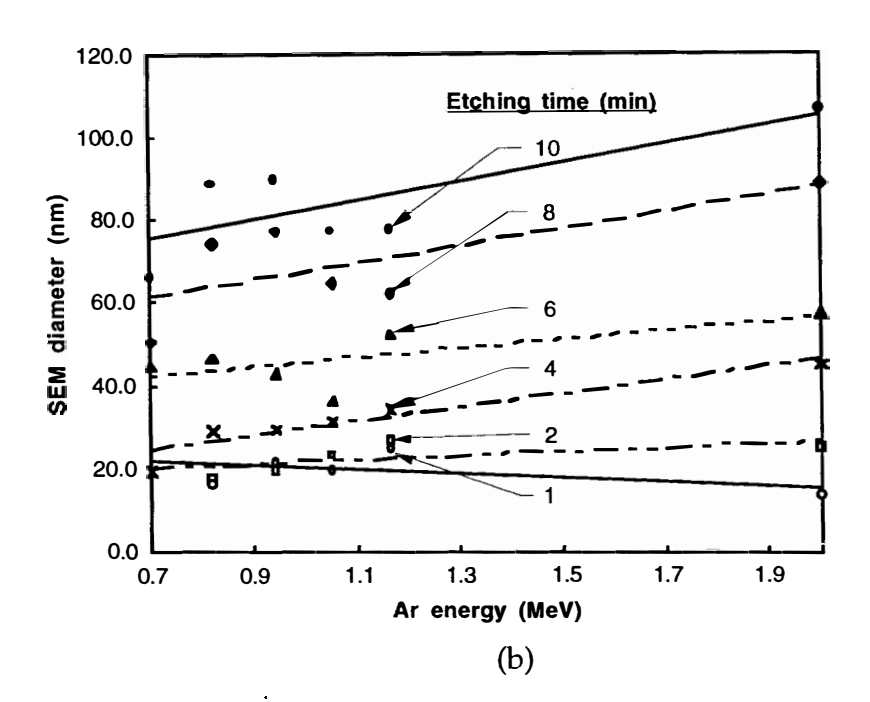
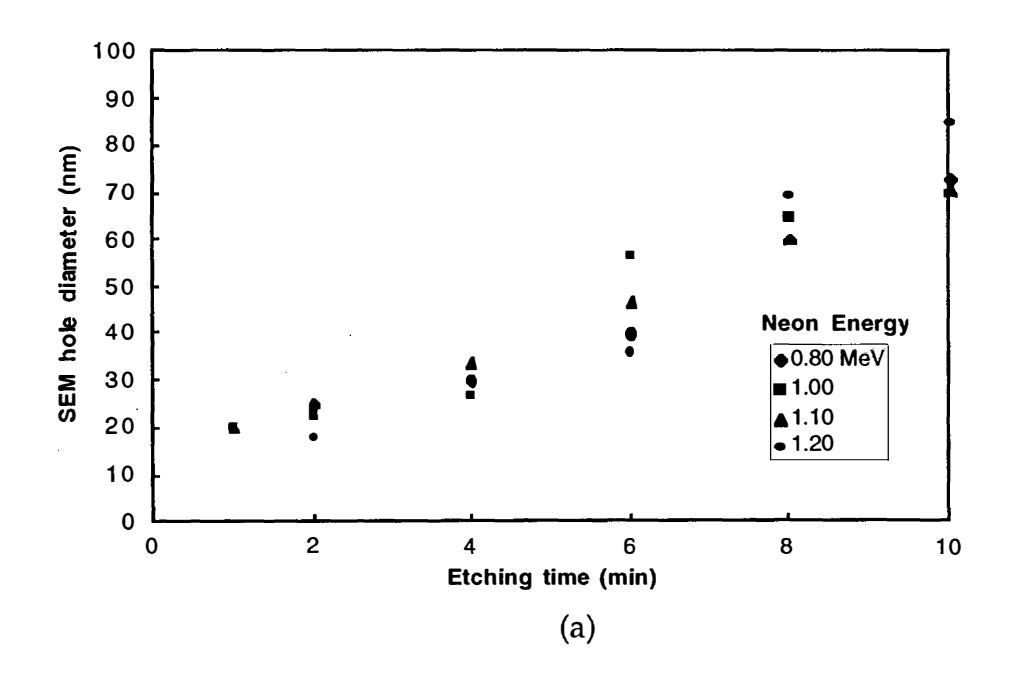


Figure 8: (a) Dependence of hole diameter on etching time with Ar ion energy as the parameter and (b) dependence of hole diameter on Ar ion energy with etching time as the parameter.



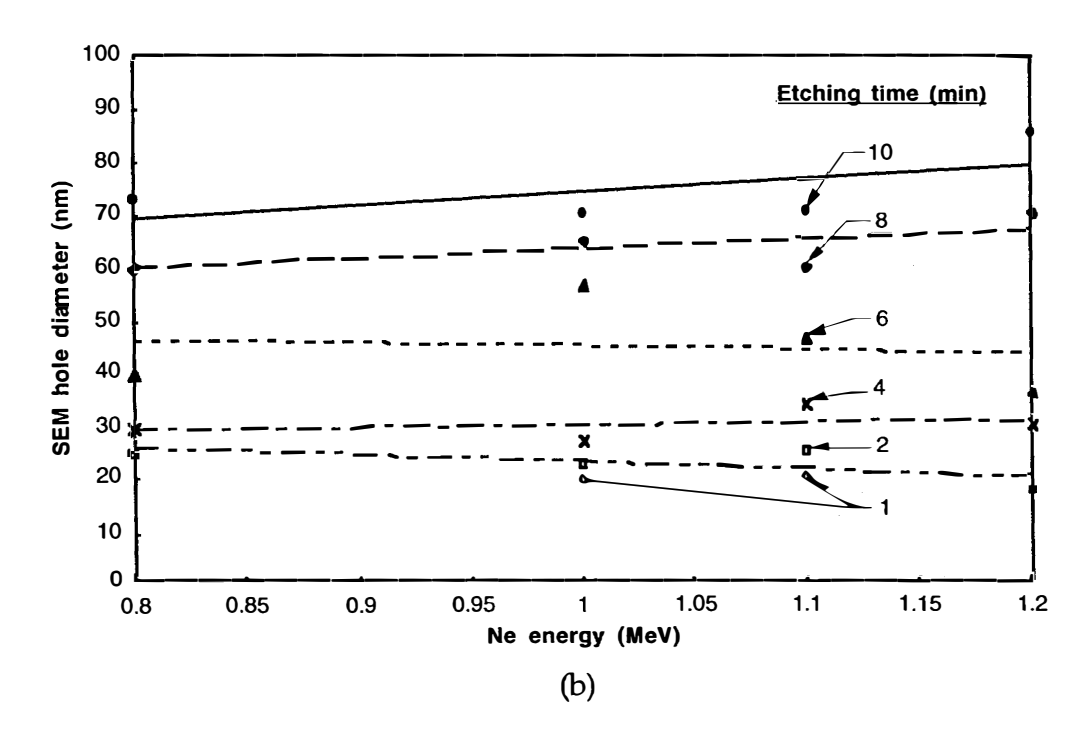
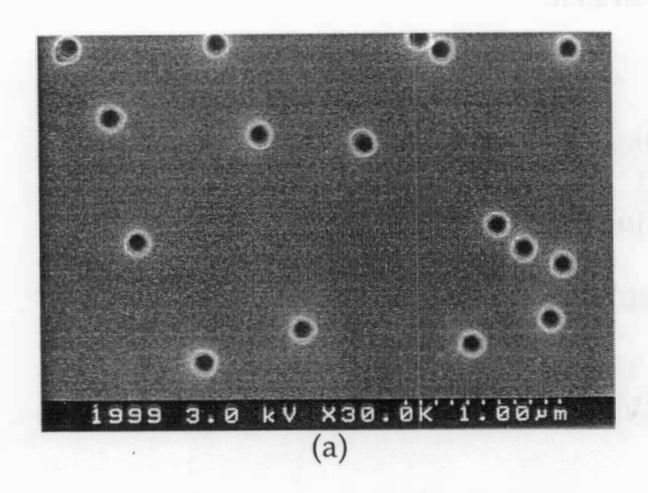
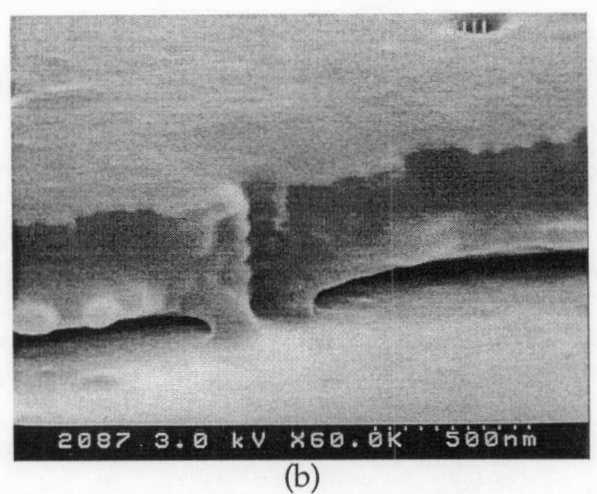


Figure 9: (a) Dependence of hole diameter on etching time with Ne ion energy as the parameter and (b) dependence of hole diameter on Ne ion energy with etching time as the parameter.





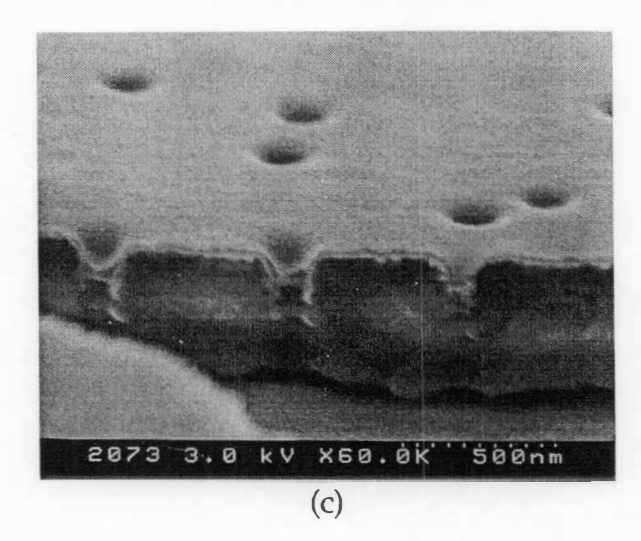


Figure 10: Holes etched in 600-nm thick polycarbonate film after irradiation with 2 MeV Ar ions and etching for 10 minutes (a) top view SEM and (b&c) cross-sectional SEMs.